Available online at www.sciencedirect.com

ScienceDirect

Journal of the European Ceramic Society 34 (2014) 1881–1892

www.elsevier.com/locate/jeurceramsoc

Toughness measurement on ball specimens. Part II: Experimental procedure and measurement uncertainties

Stefan Strobl [a,b,*], Tanja Lube [b], Oskar Schöppl [c]

[a] *Materials Center Leoben Forschung GmbH, Roseggerstraße 12, 8700 Leoben, Austria*[1]

[b] *Institut für Struktur- und Funktionskeramik, Montanuniversitaet Leoben, Peter-Tunner-Straße 5, 8700 Leoben, Austria*[2]

[c] *Research & Development Office, SKF Österreich AG, Seitenstettner Straße 15, 4401 Steyr, Austria*[3]

Received 30 October 2013; received in revised form 3 December 2013; accepted 13 December 2013

Available online 25 January 2014

Abstract

The "Surface Crack in Flexure" method is widely used for fracture toughness (K_{Ic}) determination of ceramics. In part I of the paper we developed the theoretical fundamentals to apply this procedure to ceramic balls by using the stress application as developed for the so-called "Notched ball test". The new test (SCF-NB) can be used to test spherical components without the need to cut out special specimens such as bending bars. In this work the practical part is presented including suggestions for crack introduction and specimen preparation and possible measurement errors are discussed. It is concluded that a measurement error less than ±5% is possible.

Experiments on balls and bars made from the same silicon nitride ceramic indicate that SCF-NB delivers the same K_{Ic}-values as standardised measurements on bars. Additionally, K_{Ic}-values obtained for silicon carbide, alumina and zirconia ceramics are presented. They coincide with K_{Ic}-data from the literature.

Keywords: Rolling elements; Notched ball test; Fracture toughness; Hybrid bearings; Silicon nitride

Toughness Measurement on Ball Specimens. Part II: Experimental Procedure and Measurement Uncertainties

Stefan Strobl [a,b,*], Tanja Lube [b], Oskar Schöppl [c]

[a] Materials Center Leoben Forschung GmbH, Roseggerstraße 12, 8700 Leoben, Austria[d]
[b] Institut für Struktur- und Funktionskeramik, Montanuniversitaet Leoben, Peter-Tunner-Straße 5, 8700 Leoben, Austria[e]
[c] Research & Development Office, SKF Österreich AG, Seitenstettner Straße 15, 4401 Steyr, Austria[f]

* Corresponding author at: Institut für Struktur- und Funktionskeramik, Montanuniversitaet Leoben, Peter-Tunner-Straße 5, 8700 Leoben, Austria.
Tel.: +43 3842 402 4113; fax: +43 3842 402 4102.
E-mail address: stefan.strobl@mcl.at (S. Strobl).

[d] mclburo@mcl.at, http://www.mcl.at.
[e] isfk@unileoben.ac.at, http://www.isfk.at.
[f] oskar.schoeppl@skf.com, http://www.skf.at.

Abstract

The "Surface Crack in Flexure" method is widely used for fracture toughness (K_{Ic}) determination of ceramics. In part I of the paper we developed the theoretical fundamentals to apply this procedure to ceramic balls by using the stress application as developed for the so-called "Notched ball test". The new test (SCF-NB) can be used to test spherical components without the need to cut out special specimens such as bending bars. In this work the practical part is presented including suggestions for crack introduction and specimen preparation and possible measurement errors are discussed. It is concluded that a measurement error less than ± 5 % is possible.

Experiments on balls and bars made from the same silicon nitride ceramic indicate that SCF-NB delivers the same K_{Ic}-values as standardised measurements on bars. Additionally, K_{Ic}-values obtained for silicon carbide, alumina and zirconia ceramics are presented. They coincide with K_{Ic}-data from the literature.

1. Introduction

For most of all established methods for fracture toughness determination, the specimen geometry is standardised. Prismatic flexural beams with a cross section of 3 x 4 mm² and > 40 mm in length are used in the Single Edge V-Notch Beam (SEVNB) [1], the Chevron Notch (CN) [2] or the Surface Crack in Flexure (SCF) [3] method.

The task in the present work is to measure the toughness of balls without cutting special specimens out of the balls. For that we follow the basic ideas of the SCF method [3], where a well-defined crack is made by an indent (Knoop) into surface of a prismatic beam. Then the beam is loaded in flexure until failure occurs. From the crack geometry and the failure stress the critical stress intensity factor (fracture toughness) can be determined. One of the most important advantages of SCF method is that the start defect is a real crack and not a relatively sharp notch, which is required for the validity of linear elastic fracture mechanics (LEFM) [4]. A difficulty of the SCF method is that the indentation causes a plastically deformed zone, which provokes internal stresses. This can adulterate the testing results. Therefore the plastically deformed material has to be removed – e.g. by grinding – in order to avoid a preloading of the crack tip by residual stresses and to receive a fully closed and unloaded crack in order to follow the assumptions made for the evaluation of the experiments. Standards recommend to grind-off a layer having the thickness of 1/6 of the long indentation diagonal. An alternative suggestion for the grinding depth is given in [5], which additionally ensures that the critical point (where the stress intensity factor becomes a maximum) is not at

the surface but at the deepest point of the crack where the determination of the stress intensity factor is more precise. Therefore this situation (critical point at the deepest position) is preferred. This grinding depth is approximately 1/3 of the long indentation diagonal (more precisely it depends on the crack length before grinding and other additional parameters, see in [5]).

The measurement of the crack shape is not straight forward since the crack's visibility may dependent on the material itself. The measured quantities are influenced by the operator [6] as well as by the available devices (such as optical microscopy or SEM) [7]. The SCF standard [3] contains some advices to facilitate the crack size measurement on the fracture surface. From them only fluorescent penetration dye (FPD) was used in this work. There are further methods to enhance the visibility of the crack and its detection, such as tilted indentation [3], non-fluorescent penetration dyes [8] or decoration with lead acetate [9, 10] which are not discussed in the framework of this paper.

In the literature on the SCF testing, the geometric factor defined by Newman and Raju in the late seventies of the last century is used [11, 12]. In these papers a FE-analysis of the stress field is made. But in that time, the computers were relatively slow and a coarse FE mesh had to be used to keep the calculation time manageable. In a recent paper it has been shown, that – in extreme cases – this can cause errors up to forty per cent of the determined value [5] (remark: the formula in the SCF-standard based on the work of Newman and Raju [11, 12] is fixed to a Poisson's ratio of 0.3 and a perfect semi-ellipse). Therefore a more precise solution for the geometric factor of the surface crack has been proposed, which is used for the data evaluation in this paper (see part I [13]).

In the new test a crack is introduced into the surface of a ball with an indenter. Then the plastically deformed material is ground-off and traction forces are applied to the crack using the principles of the notched ball test (NBT) [14-18]. In the NBT a notch is cut in the equatorial plane of the ball and afterwards the notch is squeezed together by introducing point loads at the poles perpendicular to the notch (see Fig. 1). This produces a very well defined stress field (Note: the NBT has been standardised recently [14]). Tensile stresses occur at the surface opposite the notch root. This stress field (maximum tensile stress σ_{NBT}) is almost uniaxial, simple to calculate and almost insensitive regarding measurement uncertainties caused by small geometry deviation and the testing setup. Furthermore, the specimen preparation is highly flexible. The needed parameters to describe the geometry of the notched

ball specimen are illustrated in Fig. 1. All together, these are good preconditions for toughness testing. For the SCF test applied to balls we use the notation SCF-NB.

The theoretical background and the equations necessary to evaluate the experiments in this work are described in detail in the first part of this paper [13], but are shortly summarised in the following: For the creation of the start defect a Knoop hardness impression is used in analogy to the standardised SCF method to introduce an approximately semi-elliptical crack into the specimen surface, where the maximum tensile stress occurs (i.e. apex of the notched ball specimen).

The removal of residual stresses by grinding-off the deformed material applied to the notched ball specimen causes a change in the specimen geometry and thus an altered stress field at the position of the crack (see Fig. 2). This has to be taken into account in the data evaluation: the maximum tensile stress in the NBT, σ_{NBT}, has to be multiplied with a correction factor, f_{Sigma}, to get the stress in the specimen after removing the plastic deformed zone: $\sigma \rightarrow f_{\mathrm{Sigma}} \cdot \sigma_{\mathrm{NBT}}$.

The fracture toughness, K_{Ic}, is determined by the fracture stress , $f_{\mathrm{Sigma}} \cdot \sigma_{\mathrm{NBT}}$, the typical crack size, a, and the geometric factor, Y. The maximum of the geometric factor Y_{MAX} along the crack front is used for K_{Ic} calculation. Note that the value and position of the maximum depends on the geometry of the notch and of the crack and can either be at the deepest point of the crack (position A, see Fig. 2) or at the intersection of the crack with the surface (position C, see Fig 2).

$$K_{\mathrm{Ic}} = \sigma Y \sqrt{a \pi} = (\sigma_{\mathrm{NBT}} f_{\mathrm{Sigma}}) Y_{\mathrm{MAX}} \sqrt{a \pi} \qquad (1)$$

The geometry of the notch (see Fig. 1) is defined via the notch width W_{N}, the notch root radius R_{N} and notch length L_{N}. The ligament thickness h is obtained by the ball diameter D minus the notch length: $h = D - L_{\mathrm{N}}$. The resulting parameters f_{Sigma} and Y were already investigated in detail in part I of this paper [13] – for a better usability they were approximated by a fitting function. The remaining parameter in Eq. 1 is the crack depth a. Generally, the crack depth a and the crack shape a/c (see Fig. 2) are measured after the test on the fracture surfaces as proposed for the SCF method. The insertion of the crack as well as its measurement are the key topics of this part of the paper. The effect of measurement errors

of the most important quantities such as crack dimensions on the resulting K_{Ic}-values will also be discussed.

To demonstrate the applicability of the method, tests were performed on balls with a diameter of about 5 mm on four different structural ceramic materials. The results were compared with test results gained with other testing methods and with literature data.

2. Materials of study

First, the new method was verified by applying it to a state of the art commercial silicon nitride ceramic (HIPed, overall ~10 wt% content of Al_2O_3 and Y_2O_3 additives). From this reference material (further called as SNRef) balls with a nominal diameter of 5 mm and standard bending bars were available. Fracture toughness was measured by the SEVNB method [1] , by the SCF method [3] and with the SCF-NB. For both SCF methods (on bars and balls) Knoop indentation loads of 7 kg and 10 kg were used. A micrograph of SNRef can be found in Fig. 3a.

Polished balls made of four other structural ceramics were supplied by the company SKF, Austria, for a feasibility study. The balls had a diameter of ~ 5.55 mm and were polished to a mean surface roughness of approximately 10 - 15 nm, which is desired for adequate rolling contact performance. The materials are: HIPed silicon nitride with overall ~6wt% Al_2O_3 and Y_2O_3 additives (SN), 99.7% alumina with MgO-SiO_2 additives (AO), sintered silicon carbide with B and C additives (SC) and Y-TZP zirconia (ZO). Micrographs of these materials are shown in Fig. 3b-e.

The mean values and standard deviations of ball diameters, hardness and the elastic properties are given in Table 1. Note that the Poisson's ratio, ν, is important for an exact data evaluation (since the stress state in the SCF-NB is slightly biaxial). It influences σ_{NBT}, f_{Sigma} and Y, which enter into the calculation of K_{Ic} in Eq. (1). Furthermore, for certain crack shapes, the Poisson's ratio affects the position along the crack front, where the geometric factor Y becomes a maximum ($Y \rightarrow Y_{MAX}$). This topic is discussed in detail in [5].

The elastic constants (e.g. Young's modulus E, Poisson's ratio ν) were measured by resonant ultrasonic spectroscopy (RUS) [19-21]. Balls in the as polished condition (= as received) were probed. Because of the almost perfect ball geometry (i.e. the balls are manufactured within very narrow tolerances), the measurement error in the elastic constants was very small (<0.5 %).

3. Sample Preparation

3.1. Silicon nitride, alumina and silicon carbide

For the conventional SCF method, standard bending beams (3 x 4 x 50 mm³) were diamond ground from larger plates. For SEVNB tests notches were manufactured into the 4 x 50 mm sides of the beam according to[1].

For the notch preparation of the NBT specimens one batch of balls (up to 30 specimens) was glued in a special guide rail and the notch with the desired depth was cut through all specimens with a diamond cutting wheel. This approach guarantees that the relevant surface area will not be damaged or pre-stressed due to sample preparation and all samples have approximately the same notch depth.

All relevant specimen dimensions (see Table 2) including the deviation of the mid-cut plane versus the equatorial plane (i.e. z-offset) were measure according to the NBT standard [14] and satisfied the requirements. One exception was the notch length with 75 to 78 % of the ball diameter. The stresses for these specimens could be evaluated using the formulas in [18] (the NBT standard is designed for a notch length of 80 ± 1 %).

After the machining of the notch a crack was produced using a Knoop indenter. For this purpose the notched ball was glued on a chamfered blade which is marginally thinner than the notch. This assembly guarantees that the plane of the semi-elliptical crack is parallel to the notch mid-plane and permits an easy and reproducible Knoop indentation. Furthermore, the successful infiltration with FPD, the indentation size measurement and the grinding-off of the plastically deformed material is simplified.

In indentation pre-studies, which will not be discussed in detail in this work, the ideal indentation load (between 0.5 kg and 30 kg) for each material regarding crack formation and crack visibility was deducted. For all indentations the same hardness tester (Zwick 3212B) and a tilt angle of 3 ° was used. An example for an indentation load of 15 kg in silicon nitride is given in Fig. 4. Remark that the radius of the ball surface may significantly influence the resulting indentation size, as well as the resulting cracks next to the indent.

According to [3, 7] the long diagonal d of the Knoop indent (see Fig. 4a) should be used to calculate the necessary depth of material removal ($\Delta h = d / 6$). In Fig. 4b a photograph of the same indent under UV-light is illustrated, where the crack length $2c_0$ before grinding is easy to determine using the FPD (cf. Fig. 4a). This initial crack length was used for the

calculation of Δh (according to [5]), which in addition ensures that the critical point is not at the surface (point C, see Fig. 2) but at the deepest point of the crack (point A, see Fig. 2).

After grinding (see Fig. 4c) the crack remains clearly visible with FPD, and this crack length $2c$ can be used for verification of the crack shape, which is needed as input for the determination of the geometric factor.

The grinding process can be controlled very precisely by comparison of the levels of blade edge and the ball apex (highest point of the ball, if the notch is aligned downwards). Δh for data evaluation is obtained by the difference of ligament thickness h before grinding and of ligament thickness h' after grinding, i.e. $\Delta h = h - h'$.

In part I of this paper [13], the numerical calculations were performed for a crack depth a in the range of 0.5 % to 6.5 % of the ball radius and the grinding depth is restricted to 2 % up to 5 % of the ball radius. If no past experience exists, the indenter load that produces suitable cracks has to be determined, for each material in pre-studies. The same material dependent problems occur with the standard SCF method in bending bars. For the present investigation, a good trade-off was HK10, which was used for the silicon nitrides, alumina and silicon carbide ceramics.

3.2. Zirconia

In the case of zirconia it was not possible to create penny-shaped cracks with a Knoop indenter, even with indentation loads up to 500 N. For this reason, a special procedure was applied according to the suggestions in the VAMAS report [7] for the SCF method and the work of Torres *et al*. [22]. With a Vickers indenter a hardness indent with a tilt angle of about 3 ° was produced in the apex of the notched ball specimen. One crack at the indentation corner was so small, that it was completely removed by the subsequent grinding procedure (see Fig. 5a). In pre-studies the indentation load of 196 N (HV20) showed the best result. A typical appearance of such a tilted Vickers indentation can be found in Fig. 5b. The left crack is significantly smaller than all others. As a minimum for the material removal Δh the half of the Vickers indent diagonal was chosen.

4. Testing Procedure

4.1. General Aspects

The testing procedure is similar to the procedure used for the conventional NBT for strength testing [14, 18]. A universal testing machine (Zwick GmbH & Co. KG, Ulm, Germany) with

two parallel anvils made of silicon nitride plates was used. The tests were performed using displacement control so that fracture occurs within 5 to 10 seconds. The maximum load (i.e. at fracture) was used to determine the fracture stress σ_{NBT} [14, 18].

After testing, the shape of the pre-crack was investigated at the fracture surfaces. The determination of the crack geometry at the fracture surface can be performed using a conventional stereo microscope with or without FPD. In the majority of cases the geometry of the crack (a and c) is easily to determine by fractographic analysis (and the use of FPD) [3, 7]. In the present work all specimens were infiltrated with FPD (WB200, RIL-Chemie) before grinding to decorate the pre-crack. We suggest to measure the crack shape directly after testing, otherwise the dye may spread further onto the rest of the fracture surface and the pre-crack dimensions are overestimated.

4.2. Silicon nitride, alumina and silicon carbide

The ideal case is illustrated in Fig. 6 for SNRef. By comparison of the $2c$ measured at the ground surface before testing (Fig. 6a) with the $2c$ measured at the fracture surface (Fig. 6b), one can estimate the reliability of the crack shape determination. Generally the FPD method works quite well for silicon nitride, silicon carbide and alumina. Swab and Quinn [23] reported so-called “precrack halos” and possibly an influence of slow crack growth in alumina, but no halos were observed at all in our studies.

4.3. Zirconia

As mentioned in a previous section in zirconia the pre-crack was created via a tilted Vickers indent. Ideally three cracks remained in the sample after material removal – an example is illustrated in Fig. 7a. The direction of the stress in the NBT (indicated with arrows) was nearly perpendicular regarding the horizontally aligned crack. After testing this crack was clearly visible at the fracture surface (see Fig. 7b): it has a kidney shape. For data evaluation it was approximated as a semi-elliptical crack.

4.4. Indentation Fracture Resistance

The significance of indentation fracture resistance [6, 8, 22, 24-32] (IFR) test results is still somewhat unclear and therefore controversially discussed. But the method is often used – especially in industry – to get a rough estimate of the fracture toughness. Thereby a Vickers indent is introduced in the material and the lengths of the cracks originating from the corners of the indent are measured. The IFR can be determined from the length of the cracks, the

indentation load, the Young's modulus and the hardness of the material. Many different equations for the evaluation of IFR tests exist, which have been calibrated to measurements in various materials. These equations may give quite different values for the IFR; K_{IFR} .

We will compare IFR test results (evaluated with two of these equations) with SCF and SEVNB test results. One is the equation of Niihara [30, 31] for penny-shaped cracks, which is also a criterion in the specification standard [33] for silicon nitride materials designated for ball bearing applications. The second equation has been proposed by Miyoshi [28]. It was developed considering a wide range of different ceramic materials and indentation loads.

We made the indents into the polished cross sections of the balls in the equatorial plane. At least 10 indents were measured for each material and each indentation load (1, 2, 5, 10, 20 and 30 kg).

5. Experimental Results

5.1. Evaluation of the SCF-NB method: fracture toughness of the reference material

The results of fracture toughness tests on SNRef are summarised in Table 3. For the SCF tests the location of the maximum value for the geometry factor Y is indicated in the case of semi-elliptical cracks. For most measurements the critical location was at the deepest point of the crack (point A, see Fig. 2). For the indentation load 10 kg on ball specimens, the maximum of the stress intensity factor occurred at the intersection of the crack with the specimen surface (point C).

The SEVNB method – evaluated according to the SEVNB standard [1] – provides a fracture toughness K_{Ic} of 5.4 ± 0.1 MPa $m^{1/2}$ that is a little lower than all other K_{Ic}-results obtained for this material.

For the SCF method the results for K_{Ic} are given in Table 3. For tests on bars the indentation loads of 7 kg and 10 kg provided a $K_{Ic} = 5.7 \pm 0.1$ and 6.0 ± 0.2 MPa $m^{1/2}$, respectively. The standard deviations of the fracture toughness data determined at different indentation loads do not overlap. As predicted for these crack shapes in [5] the fracture starts in point A.

For the SCF-NB (performed on balls), K_{Ic} was obtained according to part I [13]. In the case of the balls indented with 7 kg the maximum of the stress intensity factor was at point A and the fracture toughness was $K_{Ic} = 6.1 \pm 0.2$ MPa $m^{1/2}$. In the case of the balls indented

with 10 kg the maximum of the stress intensity factor was at point C and the fracture toughness was 6.5 ± 0.1 MPa $m^{1/2}$.

It should be noted that whether point A or C becomes critical depends on the Poisson's ratio and on geometrical details of the starter crack. In the actual case – as analysed in [5, 13] – the critical point is C if $a/c < 0.7$. This perfectly fits to the test results described in this subsection.

5.2. SCF-NB fracture toughness of four structural ceramics

Of each of the materials SN, AO, SC and ZO, six balls were used for SCF-NB testing, see Table 4. According to the theoretical prediction [5, 13] all specimens had the critical point at the surface (point C) due to the crack shape ratios of $a/c > 0.7$ (remember, the condition was $a/c < 0.7$).

All notched ball specimens made of SN were indented with 10 kg. The mean crack shape ratio is $a/c = 0.71$. Accordingly to this the stress intensity factors of point C (6.2 ± 0.1 MPa $m^{1/2}$) and point at A (5.6 ± 0.2 MPa $m^{1/2}$) were close together in the tests. The AO sample was split in two batches with 3 specimens each. One batch was indented with 5 kg and one with 10 kg that resulted in clearly different crack sizes (factor ~2). The K_{Ic} mean value for HK5 is slightly smaller than the value for HK10 but statistically indistinguishable. For all six SC notched balls an indentation load of 10 kg was used. This resulted in relatively big cracks, which showed extremely good overall measurability of the crack shape with FPD but also in a stereo microscope. Therefore, the scattering in K_{Ic} with 3.0 ± 0.3 MPa $m^{1/2}$ does not result from the measurement uncertainties of the crack depth or crack width. The K_{Ic} measurements of zirconia (ZO) resulted in 4.4 ± 0.3 MPa $m^{1/2}$.

6. Discussion

6.1. Fracture toughness results

The K_{Ic}-values of the reference material (a silicon nitride ceramic) generally tends to increase with higher indentation loads (this observation is statistically significant). A plot for SNRef of the K_{Ic}-values versus the crack length Δa is shown in Fig. 8.

Δa denotes the crack length, where crack bridging effects may occur (e.g. due to grain interlocking). For a "Surface Crack in Flexure" it holds $\Delta a = a$. In the case of the SEVNB-test fracture is most likely caused by very small (Δa < 10 µm) cracks in front of the V-notch

[36, 37]. Hence, the results of the SEVNB-tests are plotted at a crack length of 10 µm. The result of SEVNB together with the SCF values implies the existence of a rising crack resistance curve, i.e. R-curve. This behaviour is typical for commercial silicon nitrides and has already extensively studied for some special materials. The data shown in Fig. 8 are consistent R-curves published in [38].

Another explanation for the high K_{Ic}-value of the HK10 indented balls could be the position of the critical point at the surface (at point C) in contrast to all other tests. In fact the correct description of a crack intersecting the surface (at point C) is still an open question. At point C the stress singularity does not exactly follow an inverse square root law [39] (as it is supposed in LEFM) and T-stresses may become relevant [39-41]. In addition, pop-in-events – as mentioned in appendix B of the SCF standard [3] – are an unsolved uncertainty.

In order to force point A to become critical, it would be necessary to produce shallower cracks with a smaller a/c-ratio, i.e. to grind-off (a little) more material from the indented ball surface. An estimation for the minimum grinding depth for the conventional SCF method in flexure bars is given in [5], which can be analogously used for the NBT, by approximating bar's thickness with the thickness of the ligament of the notched ball specimen. For details see [42].

In the last column of Table 4 K_{Ic} values from literature are given for all materials (SN, AO, SC and ZO) for comparison. All these results have been measured with the SCF method on bars under similar indentation loads as used in this work. Also the microstructures are comparable – only the alumina ceramic has a smaller mean grain size than the AO ceramic. All K_{Ic} references fit well to the results in this work considering standard deviation.

6.2. Measurement error

For each new testing method the error analysis is a key element to understand how reliable, reproducible and sensitive the obtained result is regarding errors of the input data. In the discussed case the measurement of the crack shape is a crucial topic for the fracture toughness evaluation with surface cracks in the SCF method. Therefore, not only the reproducibility of surface cracks but also the measurement error in the crack length and the crack width is an important issue to be discussed.

In Fig. 9a a comparison of crack dimensions measured with i) grazing incident light and ii) with FPD is shown. The cracks in alumina and zirconia were not measureable on the fracture surface without penetration dye, so no reference values are available for these

materials. Hence, only the SN, SC and SNRef are discussed. The dashed lines in Fig. 9 indicate the ± 10 % confidence intervals. As one can see, most of the data points are within ± 10 % deviation. Large cracks seem to be measured longer without FPD. This means that the crack dimensions are not overestimated using FPD. The FPD measurements were repeated one day later and the same results were obtained.

As mentioned before, the full crack width $2c$ can be determined directly before fracture at the polished surface, preferably with FPD. This procedure is supposed to be more precise and reproducible than measurement of the crack width on the fracture surface. The results are illustrated in Fig. 9b – all measurements are within a deviation of ± 10 % for the investigated materials but the measurements at the fracture surface give tentatively (slightly) larger crack length values than the measurements at the specimens surface. Conclusions for the crack shape measurements with the used penetration dye are:

i) For fine grained materials the use of FPD is very useful, especially considering the ease of use, experience of the operator and time consumption. Ideally, the measurement precision does not suffer.
ii) In materials such as alumina the crack shape is very difficult to measure without FPD.
iii) The measurement of the crack at the polished surface is only possible with FPD and helps to keep the measurement uncertainties low (< 5 %).
iv) no scanning electron microscope analysis is necessary to obtain accurate crack shape geometries.

According to Eq. (1), K_{Ic} depends on three factors. The errors in σ_{NBT} and f_{Sigma} were already discussed in the first part of this paper [13] – both are typically less than 1-2 %. The remaining factors are mainly affected by the crack size and shape. In addition, the critical point for the start of crack propagation may change abruptly (depending whether Y_{MAX} is in point A or in point C). As a consequence, we introduce a new variable $Y' = Y_{\mathrm{MAX}}\sqrt{a\,\pi}$. for the error analysis. This approach enables us to investigate the influence of errors in the crack geometry, i.e. the error in the crack depth a_{err} and in the crack width c_{err} simultaneously. The influence of other geometrical parameters and of the Poisson's ratio as well as their interaction with the crack shape deviation on the determination of the stress intensity factor is small (much lower than 1 %) and can be neglected.

The geometrical factor Y is unit independent and was calculated in part I for all specimen geometries, which are relevant in practice. With Y', the overall effect of crack dimension measurement errors on error in K_{Ic} for a characteristic specimen can be investigated. Furthermore, the relative influence of a given a_{err} is stronger for small cracks than for big cracks. As reference geometry of the notched ball specimen, the following parameters were chosen for the error analysis: $D = 5$ mm, $L_N = 4$ mm, ($\rightarrow h = 1$ mm), $W_N = 0.5$ mm, $R_N =$ 0.125 mm, $\Delta h = 100$ µm and $\nu = 0.3$. To cover all measured crack geometries in the investigated materials (see Table 3 and Table 4), two representative crack depths ($a =$ 100 µm and $a = 200$ µm) and two extrema in the crack shapes ($a/c =$ 0.5 and $a/c =$ 1) were investigated.

An error in the measurement can occur in four different kinds: only in a, only in c or in both (in the same direction or in the opposite direction, respectively). These four cases are plotted in Fig. 10a for $a/c =$ 1 with $a =$ 100 µm. If $a_{err} = 0$ and only c is incorrect, $\Delta Y'$ is nearly zero (which is equivalent to zero error in K_{Ic}). For a measurement error of ± 20 µm in the crack dimensions a or c, $\Delta Y'$ rises up to 10 %.

For a shallow crack ($a/c =$ 0.5) with $a = 100$ µm (Fig. 10b) the error for ± 20 µm (in either a or c) is below 4 % for the geometric factor in all cases, that are representative for the SN and SNRef specimens. One reason for this low error could be that the geometric factor is critical in point A for most of the plotted data points. The curves are discontinuous and Y_{MAX} switches to point C on the right hand side of the graph.

For deeper cracks ($a = 200$ µm) point C always remains the critical one, as one can see in Fig. 10c and d. Again a measurement error exclusively in c has almost no effect on K_{Ic}. When a_{err} is about $+20$ µm and c_{err} is about -20 µm, $\Delta Y'$ increases above 10 % for $a/c = 1$. In all other configurations the resulting error stays below 5-6 %. This can be quantified as the typical error in alumina and silicon carbide with 10 kg indents resulting from errors in the crack shape determination.

Three points can be concluded from this error analysis:

i) The error in K_{Ic} due to errors in crack geometry measurements is typically smaller than 10 %. For shallow cracks the resulting error is smaller than 5 %, which is an additional argument to create shallow cracks.

ii) The accurate determination of a is significantly more important than that of c (see dashed lines in Fig. 10).

6.3. Comparison IFR with fracture toughness test results

Tests on the SNRef material: For all used indentation loads cracks at the corners of the indents occurred, which could be used for the determination of the indentation fracture resistance, K_{IFR}. Following the suggestion of [27] the test results are plotted in Fig. 8 versus the effective crack length $\Delta a = c_V - d_V / 2$. c_V is the distance between indent center and crack tip, and d_V the indent diagonal. K_{IFR}-results for all evaluated loads are illustrated as lines showing a slightly increase with the crack length. If the K_{IFR}-values are evaluated using the equation of Miyoshi, the values are about 6 MPa $m^{1/2}$. They are in good agreement with the SCF results. If the evaluation is made using the equation of Niihara (and therewith following the evaluation recommended in ASTM F 2094-08), the values are about 7.5 MPa $m^{1/2}$ and do not fit the measured fracture toughness values.

Tests on four structural ceramic materials (SN, AO, SC and ZO): The K_{IFR} test results shown in Table 4 and are plotted in Fig. 11. The K_{Ic}-values are shown on the left hand side of the diagram without information about the crack length (see Table 4).

In the case of SN the K_{IFR} values were determined on indents made with a load of 1 kg to 30 kg. The indents in the AO and SC materials were only evaluable, if loads between 2 kg and 5 kg were applied. The other tests were rejected due to the influence of big pores, material break-outs and lateral cracks around the indents.

For ZO the scatter of the data was very large. As shown in Fig. 7b at an indentation load of 20 kg Palmqvist cracks were produced on each corner of the indent. This is in accordance with the work of Kaliszewski *et al*. [26]. They found that half-penny cracks are created in zirconia (Y-TZP) with loads above 50 kg. The used IFR-formulas are only applicable for half-penny cracks and deliver erroneous values for other crack geometries. In our case the cracks had a kidney shape and the K_{IFR} data evaluation may become meaningless.

If the tests were evaluated with the Miyoshi equation the SN data nicely correlate with our fracture toughness values for higher indentation loads, but data evaluated with the Niihara equation do not. In the case of AO the K_{IFR} do not correlate with fracture toughness values irrespective which evaluation equation is used (neither Niihara nor Miyoshi). K_{IFR}-values of

SC do not depend on indentation load. The Miyoshi formula gives K_{IFR} values which correlate with our K_{Ic} test results.

The results of the IFR method can be summarised as following: (i) The commonly used IFR Niihara evaluation does not match the fracture toughness of all investigated materials, even of silicon nitride. (ii) In two materials (silicon carbide and silicon nitride) the Miyoshi formula fits the fracture toughness within the experimental standard deviation. (iii) The IFR method generally depends on the indentation load. An overestimation by the factor of 2.5 (in zirconia) is possible. (iv) Due to the formation of different crack patterns (Penny-shaped cracks, lateral cracks, Palmqvist cracks, etc.) the evaluation procedure for IFR may become meaningless. In summary IFR-measurements should not be used for the estimation of fracture toughness.

7. Conclusions

In part I of this paper [13] the theoretical analysis of the SCF method applied to notched ball specimen (SCF-NB) was conducted. In this second part the method is applied to several structural ceramics to demonstrate the experimental applicability. The following conclusion can be drawn:

- The SCF method delivers the same testing results whether it is applied to beams (as described in standards) or to balls (SCF-NB).
- The data determined with the SCF-NB test also coincide with results measured with other methods and with literature data.
- The developed evaluation procedure proved to be suitable. For example it could be shown that it can be predicted whether the highest stress intensity factor is at the position A or C of the crack front.
- It is recommended to prepare the specimens in such a way that point A will become critical. This can simply be made by grinding a little more of the indented volume away, so that the ration a/c becomes less than 0.7 (shallower cracks). In point A the measurement uncertainties are much smaller than in C.
- The use of fluorescent penetration dye (FPD) is useful to measure the crack size.
- The measurements of the indentation fracture resistance showed, that the gained data strongly depend on the used evaluation method and are not reliable. It is

recommended not to use indentation fracture resistance measurement for fracture toughness estimations.

The practical effort and time consumption should also be considered. The production of notched balls specimen directly from the balls for strength testing is generally faster than the production of a (standard) bending beam from a ball. The effort for the crack introduction, measurement, grinding procedure and testing is very similar to the effort in conventional SCF-testing and both methods have generally the same advantages and disadvantagous. With the SCF-NB test also small spherical components can be tested, which seems not to be feasible with other reliable measurement techniques. A lower limit for the ball diameter for the preparation of a notched ball specimen is around 3 mm. Below that size the alignment of the crack and the cutting of the notch may cause considerable geometrical deviations; possibly other notching procedures can solve this problem.

A short comment to the used evaluation equations should be given. In this work, the solutions for stress fields and stress intensity factors described in part I of the paper [13] are used. In the standards the Newman and Raju equation [12] is used which is less precise than our equation. In the case of the measurements presented in this paper the differences between both equations are relatively small (between 0 to 7 %), but it should be recognised, that depending on the Poisson's ratio of the investigated material and the crack geometry much higher differences may arise. This fact is even more relevant if the critical point at the crack front is point C.

In summary it can be stated, that the new method to determine the fracture toughness in the surface of balls can be recommended for wider use. Especially in the case of bearing balls it could be a good solution for a fair comparison between different materials.

Acknowledgement

Financial support by the Austrian Federal Government (in particular from Bundesministerium für Verkehr, Innovation und Technologie and Bundesministerium für Wirtschaft, Familie und Jugend) represented by Österreichische Forschungsförderungsgesellschaft mbH and the Styrian and the Tyrolean Provincial Government, represented by Steirische Wirtschaftsförderungsgesellschaft mbH and Standortagentur Tirol, within the framework of the COMET Funding Programme is gratefully acknowledged.

Literature

[1]. ISO 23146. Fine ceramics (advanced ceramics, advanced technical ceramics) - Test methods for fracture toughness of monolithic ceramics - Single-edge V-notch beam (SEVNB) method. 2008.

[2]. ISO 24370. Fine ceramics (advanced ceramics, advanced technical ceramics) - Test method for fracture toughness of monolithic ceramics at room temperature by chevron-notched beam (CNB) method. 2005.

[3]. ISO 18756. Fine ceramics (advanced ceramics, advanced technical ceramics) - Determination of fracture toughness of monolithic ceramics at room temperature by the surface crack in flexure (SCF) method. 2003.

[4]. Munz D, Fett T. Ceramics - Mechanical Properties, Failure Behaviour, Materials Selection. Berlin: Springer; 2001.

[5]. Strobl S, Supancic P, Lube T, Danzer R. Surface Crack in Tension or in Bending - A Reassessment of the Newman and Raju Formula in Respect to Fracture Toughness Measurements in Brittle Materials. Journal of the European Ceramic Society 2012;32:1491-501.

[6]. Miyazaki H, Hyuga H, Yishizawa Y-i, *et al.* Fracture Toughness Test of Silicon Nitrides with Different Microstructures using Vickers Indentations. Ceramic Engineering and Science Proceedings 2008;28:433-42.

[7]. Quinn GD, Kübler J, Gettings RJ. Fracture Toughness of Advanced Ceramics by the Surface Crack in Flexure (SCF) Method: A VAMAS Round Robin. VAMAS Report No. 17. Report 1994.

[8]. Miyazaki H, Hyuga H, Yishizawa Y-i, *et al.* Crack Profiles under a Vickers Indent in Silicon Nitride Ceramics with Various Microstructures. Ceramics International 2010;36:173-9.

[9]. Jones SL, Norman CJ, Shahani R. Crack-Profile Shapes Formed Under a Vickers Indent Pyramid. Journal of Materials Science Letters 1987;6:721-3.

[10]. Lube T. Indentation Crack Profiles in Silicon Nitride. Journal of the European Ceramic Society 2001;21:211-8.

[11]. Newman JC, Raju IS. Analysis of Surface Cracks in Finite Plates under Tension or Bending Loads NASA. Report TP-1578; 1979.

[12]. Newman JC, Raju IS. An Empirical Stress-Intensity Factor Equation for the Surface Crack. Engineering Fracture Mechanics 1981;15:185-92.

[13]. Strobl S, Supancic P, Lube T, Danzer R. Toughness measurement on ball specimens. Part I: Theoretical analysis. Journal of the European Ceramic Society 2012;32:1163-73.

[14]. ÖNORM M 6341. Rolling Bearings — Ceramic bearing balls — Determination of the strength — Notched ball test. 2013.

[15]. Supancic P, Danzer R, Harrer W, *et al.* Strength Tests on Silicon Nitride Balls. Key Engineering Materials 2009;409 193-200.

[16]. Supancic P, Danzer R, Wang Z, *et al.* The Notched Ball Test - A New Strength Test for Ceramic Spheres. 9th International Symposium on Ceramic Materials and Components for Energy and Environmental Applications, Shanghai: The American Ceramic Society; 2009, p. 67-75.

[17]. Supancic P, Danzer R, Witschnig S, Polaczek E. The Strength of Ceramic Balls - The Notched Ball Test. 18th European Conference on Fracture, Dresden: 2010.

[18]. Supancic P, Danzer R, Witschnig S, *et al.* A new Test to determine the Tensile Strength of Brittle Balls - The Notched Ball Test. Journal of the European Ceramic Society 2009;29:2447-59.

[19]. EN 15335. Advanced Technical Ceramics - Ceramic Composites - Determination of Elastic Properties by Resonant Beam Method up to 2000 °C. 2007.
[20]. Lins W, Kaindl G, Peterlik H, Kromp K. A novel Resonant Beam Technique to determine the Elastic Moduli in Dependence on Orientation and Temperature up to 2000°C. Review of Scientific Instruments 1999;70:3052-8.
[21]. Migliori A, Sarrao JL. Resonant Ultrasonic Spectroscopy. New York, NY: Wiley Interscience; 1997.
[22]. Torres Y, Casellas D, Anglada M, Llanes L. Fracture Toughness Evaluation of Hardmetals: Influence of Testing Procedure. International Journal of Refractory Metals and Hard Materials 2001;19:27-34.
[23]. Swab JJ, Quinn GD. Effect of Precrack "Halos" on Frature Toughness Determined by the Surface Crack in Flexure Method. Journal of the American Ceramic Society 1998;81:2261-8.
[24]. Anstis GR, Chantikul P, Lawn BR, Marshall DB. A Critical Evaluation of Indentation Techniques for Measuring Fracture Toughness: I, Direct Crack Measurements. Journal of the American Ceramic Society 1981;64:533-8.
[25]. ISO 14627. Fine ceramics (advanced ceramics, advanced technical ceramics) - Test method for fracture resistance of silicon nitride materials for rolling bearing balls at room temperature by indentation fracture method. 2012.
[26]. Kaliszewski MS, Behrens G, Heuer AH*, et al.* Indentation Studies on Y_2O_3-stabilized ZrO_2: I, Development of Indentation-Induced Cracks. Journal of the American Ceramic Society 1994;77:1185-93.
[27]. Miyazaki H, Hyuga H, Hirao K, Ohji T. Comparison of Fracture Resistance as Measured by the Indentation Fracture Method and Fracture Toughness determined by the Single-Edge-Precracked beam Technique using Silicon Nitride Ceramics with Different Microstructures. Journal of the European Ceramic Society 2007;27:2347-54.
[28]. Miyazaki H, Hyuga H, Yishizawa Y-i*, et al.* Relationship between Fracture Toughness determined by Surface Crack in Flexure and Fracture Resistance measured by Indentation Fracture for Silicon Nitride Ceramics with Various Microstructures. Ceramics International 2009;35:493-501.
[29]. Miyazaki H, Yoshizawa Y-i, Hirao K, Ohji T. Indentation Fracture Resistance Test Round Robin on Silicon Nitride Ceramics. Ceramics International 2010;36:899–907.
[30]. Niihara K, Morena R, Hasselman DPH. Further Reply to "Comments on 'Elastic/Plastic Indentation Damage in Ceramics: The Median/Radial Crack System' ". Journal of the American Ceramic Society 1982;65:C-116.
[31]. Niihara K, Morena R, Hasselman DPH. Evaluation of K_{Ic} of Brittle Solids by the Indentation Method with Low Crack-to-Indent Ratios. Journal of Materials Science Letters 1982;1:13-6.
[32]. Quinn GD, Bradt RC. On the Vickers Intentation Fracture Test. Journal of the American Ceramic Society 2007;90:673-80.
[33]. ASTM F 2094. Standard Specification for Silicon Nitride Bearing Balls. American Society for Testing and Materials; 2008.
[34]. Park J-K, Yasuda K, Matsuo Y. Effect of Crosshead Speed on theFracture Toughness of Soda-lime Glass, Al_2O_3 and Si_3N_4 Ceramics determined by the Surface Crack in Flexure (SCF) Method. Journal of Materials Science 2001;36:2335-42.
[35]. Quinn GD, Salem JA. Effect of Lateral Cracks on Fracture Toughness determined by the Surface-Crack-in-Flexure-Method. Journal of the American Ceramic Society 2003;85:873-80.
[36]. Damani R, Gstrein R, Danzer R. Critical Notch Root Radius in SENB-S Fracture Toughness Testing. Journal of the European Ceramic Society 1996;16:695-702.

[37]. Damani R, Schuster C, Danzer R. Polished Notch Modification of SENB-S Fracture Toughness Testing. Journal of the European Ceramic Society 1997;17:1685-9.
[38]. Fünfschilling S, Fett T, Hoffmann MJ*, et al.* Bridging Stresses from R-Curves of Silicon Nitrides. Journal of Materials Science Letters 2009;44:3900-4.
[39]. Anderson TL. Fracture Mechanics - Fundamentals and Applications. Boca Raton FL: CRC Press; 2005.
[40]. Fett T. Stress Intensity Factors - T-Stresses - Weight Functions (IKM 50). Karlsruhe: KIT Scientific Publishing; 2008.
[41]. Fett T. Stress Intensity Factors - T-Stresses - Weight Functions. Supplement Volume (IKM 55). Karlsruhe: KIT Scientific Publishing; 2009.
[42]. Lube T, Witschnig S, Supancic P. Fracture Toughness of Ceramic Balls. 18th European Conference on Fracture, Dresden: 2010.

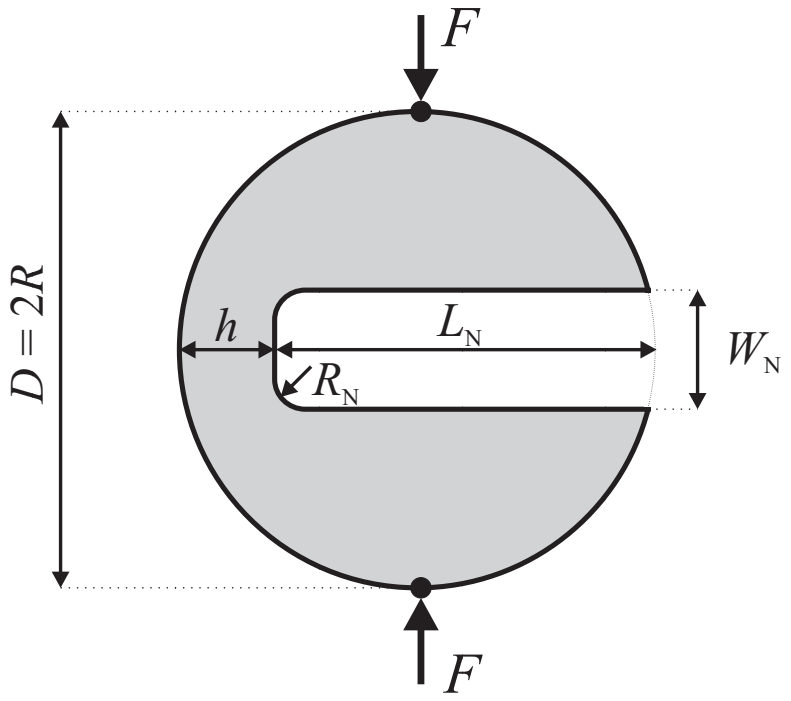

Fig. 1: Specimen in the notched ball test. The notch is defined by the length L_N, the width W_N and the fillet radius R_N of the notch. In the equatorial plane remains a ligament having the shape of a segment of a circle with the thickness $h = D - L_N$.

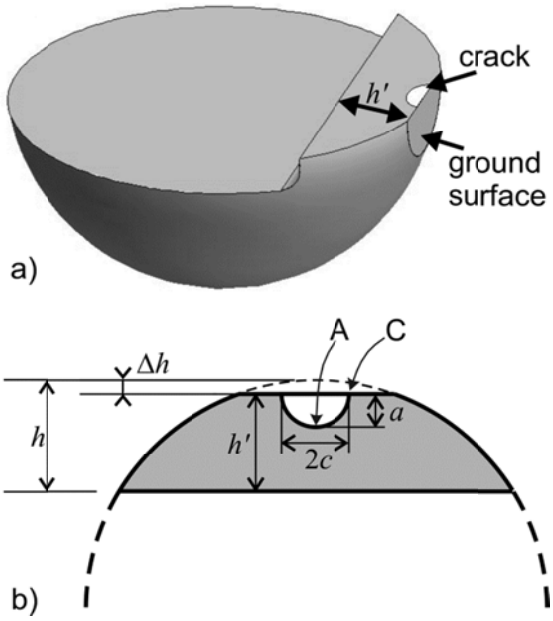

Fig. 2: Geometric situation in the fracture toughness test for balls. Shown is a half model of a notched ball with a semi-elliptical crack (white). The plastically deformed material is still removed (e.g. by grinding). The remaining ligament thickness is $h' = h - \Delta h$. Also shown are the positions A and C, where the crack may start growing.

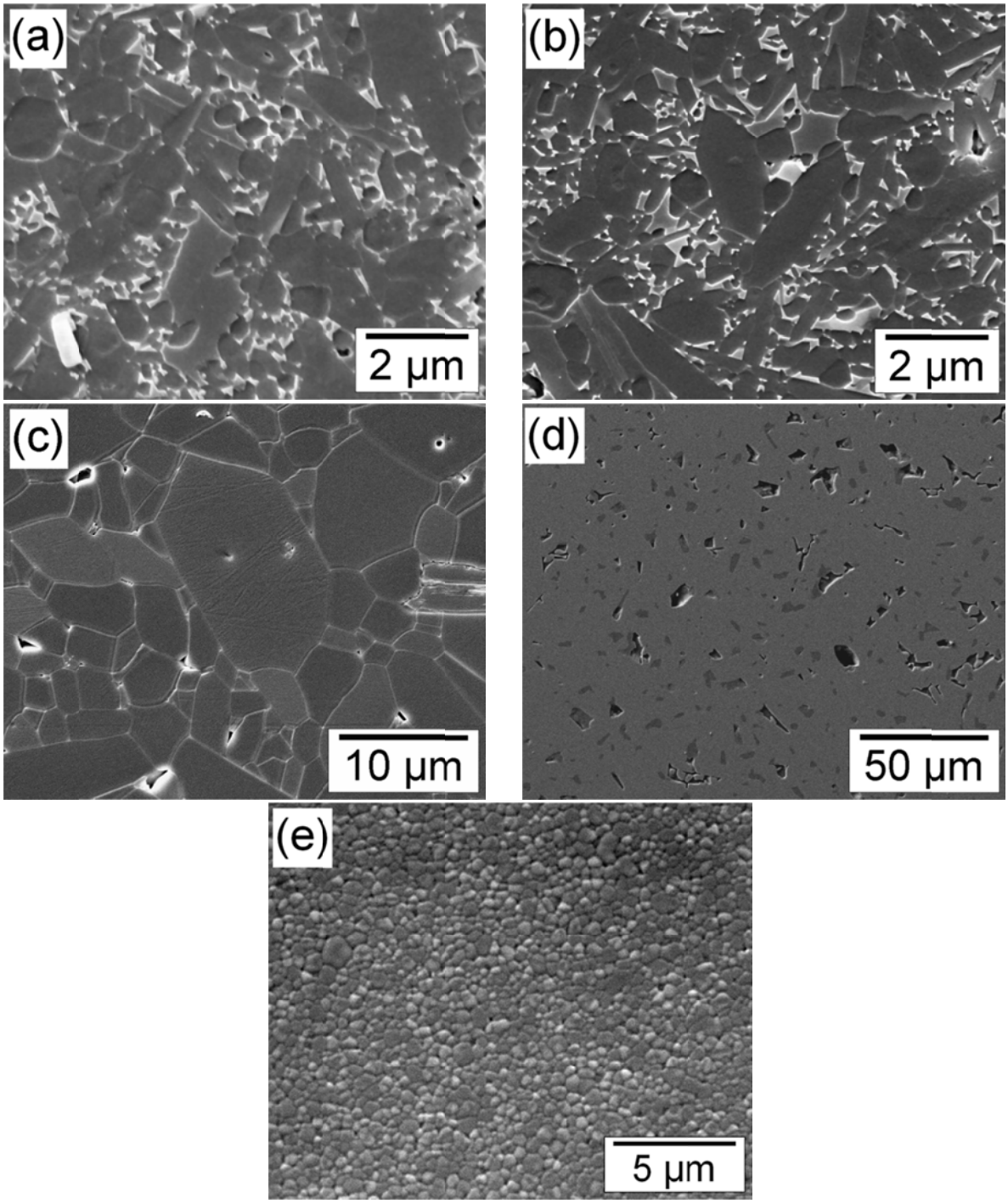

Fig. 3: SEM micrographs of all investigated materials: a) SNRef – silicon nitride, b) SN – silicon nitride, c) AO – alumina, d) SC – silicon carbide and e) ZO – zirconia.

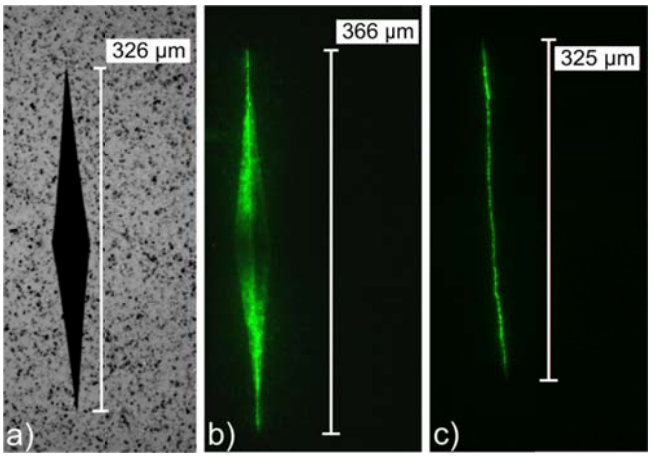

Fig. 4: HK15 Knoop indent in SNRef. a) before grinding, b) before grinding with fluorescentic pentration dye (FPD) and under UV-light and c) after grinding-off of the plastically deformed zone with FPD and under UV-light.

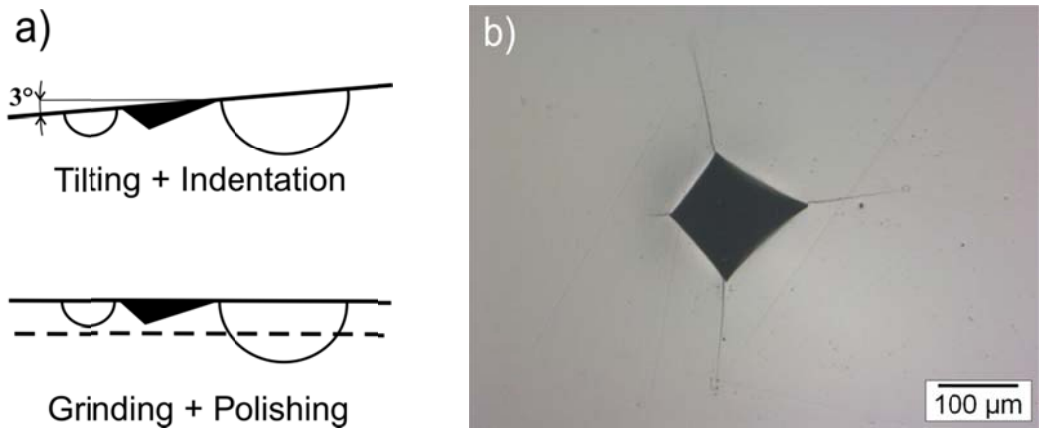

Fig. 5: Preparation method according to [22] for introduction of a surface crack in zirconia. a) schematic procedure, b) example for ZO (HV20).

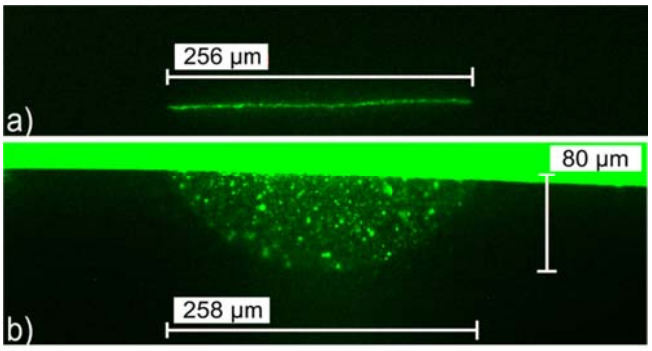

Fig. 6: Crack shape determination in SNRef (HK7) with FPD and UV light. a) full crack width 2*c* measured at the original surface (before fracture) and b) crack depth *a* and full crack width 2*c* measured at the fracture surface.

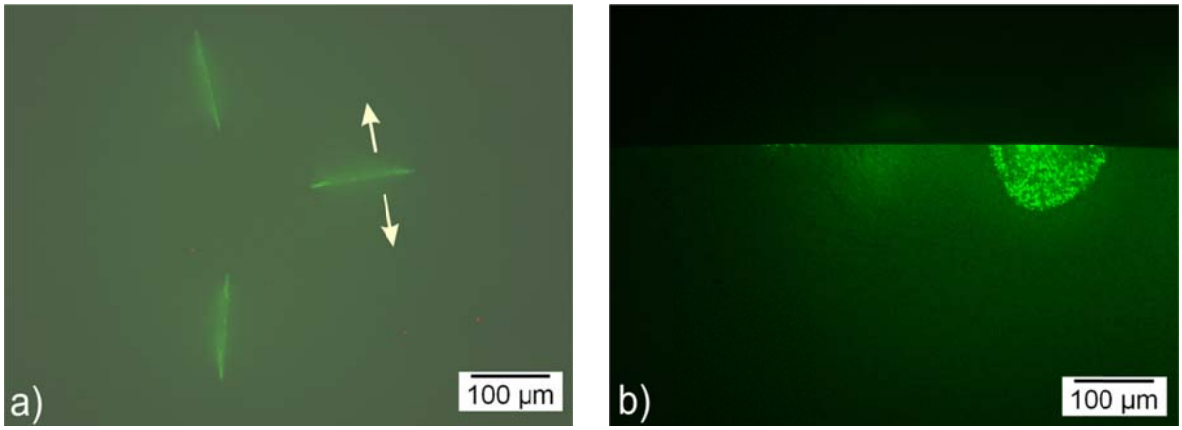

Fig. 7: Insertion of a crack via tilted Vickers Indent in the material ZO (HV20). a) after grinding at the surface with FPD, the arrows indicate the direction of the first principal stress in the NBT, b) Crack shape determination at the fracture surface with FPD.

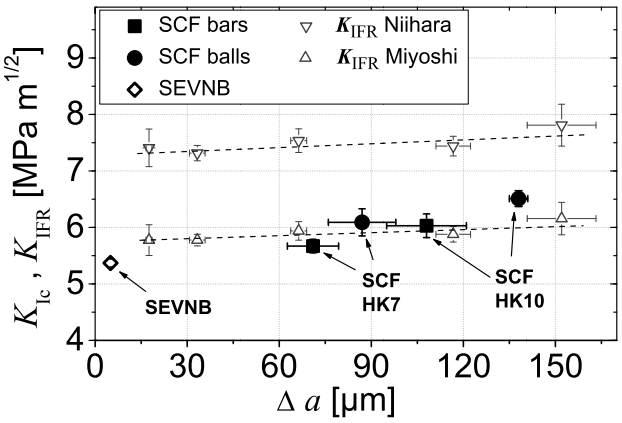

Fig. 8: Measurements of the fracture toughness K_{Ic} of SNRef using different testing methods: Measurements with the SCF method on bars (squares) and balls (circles) and results determined with the SEVNB method (open diamond). Also shown are fracture resistance measurements, K_{IFR}, evaluated according to the equations of Niihara (downwards triangles) and Miyoshi (upwards triangles).

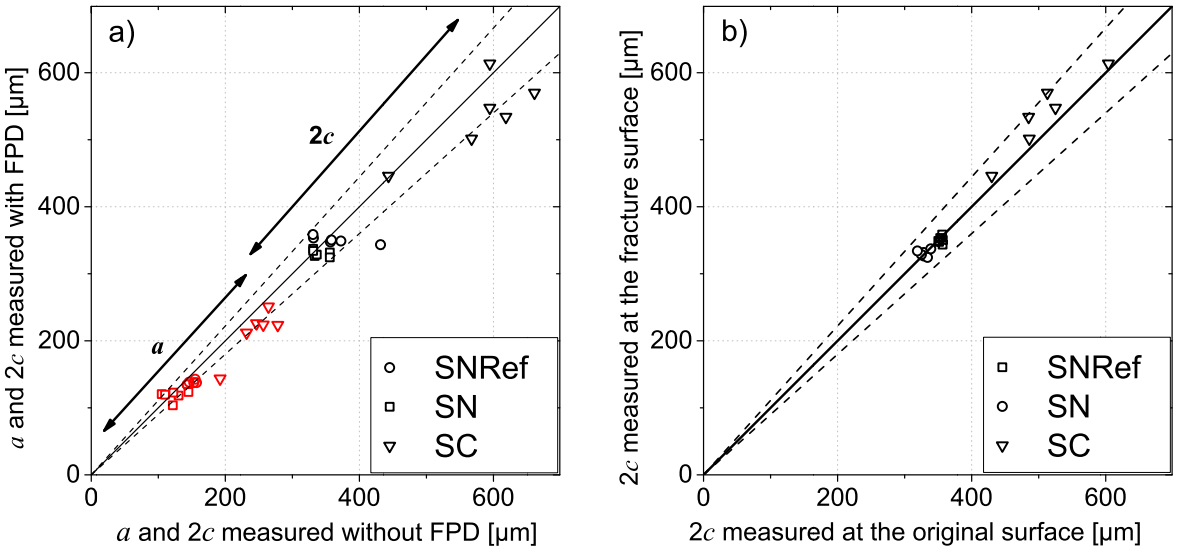

Fig. 9: a) Comparison of the crack shape parameter a and c measured at the fracture surface with FPD vs. stereo microscope measurements without FPD, b) comparison of full crack width $2c$ measured at the fracture surface vs. specimens surface (before fracture).

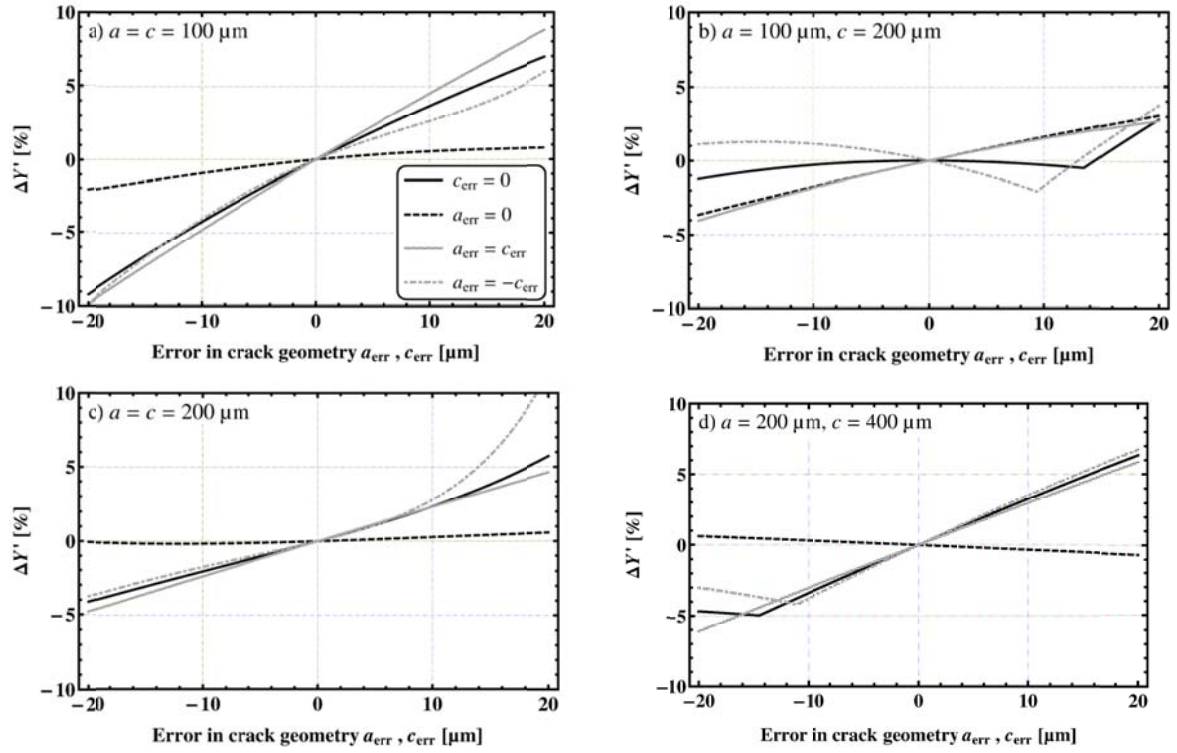

Fig. 10: Influence of crack shape measurement errors a_{err} and c_{err} on the accuracy of the (modified) geometric factor Y'. a) small crack and $a/c = 1$, b) small crack and $a/c = 0.5$, c) large crack and $a/c = 1$, d) large crack and $a/c = 0.5$.

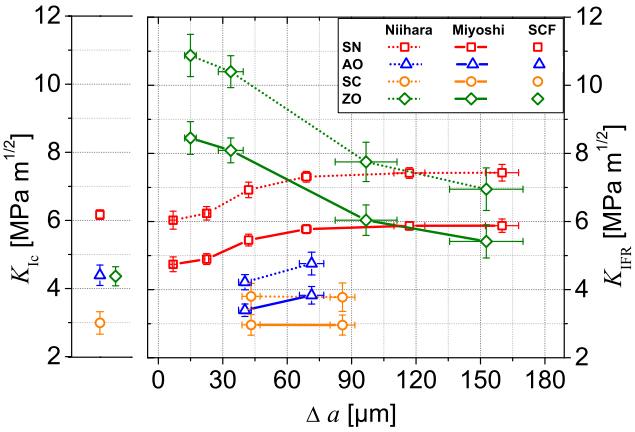

Fig. 11: Indentation fracture resistance versus effective crack length for four structural materials (SN, AO, SC and ZO). On the left hand side the K_{Ic} results (measured with the modified SCF method on balls) is plotted. The indentation fracture resistance, K_{IFR}, was evaluated using the equations of Niihara [31] and Miyoshi [28] respectively.

Table 1: Properties of the investigated ball materials.

Short name	**SNRef**	**SN**	**AO**	**SC**	**ZO**
Material	Silicon nitride	Silicon nitride	Alumina	Silicon carbide	Zirconia
Ball diameter [mm]	4.999 ± 0.001	5.550 ± 0.001	5.555 ± 0.001	5.554 ± 0.001	5.555 ± 0.001
Hardness (HV5)	1585 ± 29	1627 ± 44	1611 ± 66	2274 ± 128	1283 ± 13
Young's modulus [GPa]	306 ± 4	306.4 ± 0.1	386.6 ± 0.1	389.9 ± 0.1	217.5 ± 0.1
Poisson's ratio	0.268 ± 0.005	0.269 ± 0.001	0.234 ± 0.001	0.160 ± 0.001	0.332 ± 0.001

Table 2: Characteristic dimensions of notched balls specimen for fracture toughness tests. The data are mean values of sets of 5 to 6 specimens.

	SNRef	**SN**	**AO**	**SC**	**ZO**
Notch root radius R_N [µm]	155	234	285	256	250
Notch width W_N [µm]	628	609	691	641	628
Notch length L_N [µm]	3910 ± 2	4234 ± 2	4206 ± 4	4214 ± 8	4250 ± 3
z-offset [µm]	15 ± 7	14 ± 2	2 ± 1	5 ± 4	24 ± 2

Table 3: Results of fracture toughness measurements for SNRef on prismatic bars and balls.

specimen type / SCF indentation load	Location of Y_{MAX}	No. of samples	a [µm]	c [µm]	a / c [1]	K_{Ic} [MPa m$^{1/2}$]
Bar (SEVNB)		6				5.4 ± 0.1
Bar (SCF) / 7 kg	A	5	71 ± 8	125 ± 5	0.57	5.7 ± 0.1
Bar (SCF) / 10 kg	A	6	108 ± 13	158 ± 7	0.68	6.0 ± 0.2
Ball (SCF) / 7 kg	A	6	87 ± 11	131 ± 5	0.66	6.1 ± 0.2
Ball (SCF)/ 10 kg	C	6	138 ± 3	177 ± 1	0.78	6.5 ± 0.1

Table 4: Results of fracture toughness measurements with the modified SCF method on balls for SN, AO, SC and ZO materials.

material / SCF indentation load	Location of Y_{MAX}	No. of specimens	a [µm]	c [µm]	a / c [1]	K_{Ic} [MPa m$^{1/2}$]	K_{Ic} Literature [MPa m$^{1/2}$]
SN / HK10	C	6	118 ± 7	165 ± 2	0.71	6.2 ± 0.1	6.2 ± 0.2 [28]
AO / HK5	C	3	125 ± 34	155 ± 40	0.81	4.3 ± 0.3	4.0 ± 0.2 [34]
AO / HK10	C	3	241 ± 25	274 ± 33	0.88	4.5 ± 0.1	--
SC / HK10	C	6	216 ± 32	268 ± 29	0.81	3.0 ± 0.3	2.6 - 3.0 [35]
ZO / HV20	C	6	69 ± 17	69 ± 10	1.00	4.4 ± 0.3	4.4 ± 0.4 [7]